# Phase Noise Estimation in Full-Duplex Orthogonal Frequency Division Multiplexing Systems

Fan-Shuo Tseng,[+] Tsang-Yi Wang,[*] Chun-Tao Lin,[†] and Chun-Cheng Su[#]
[*+#]Institute of Communications Engineering, National Sun Yat-sen University, Kaohsiung, Taiwan
[†]Department of Electrical Engineering, National Taipei University of Technology, Taipei, Taiwan
Email: fs.tseng@mail.nsysu.edu.tw; tcwang@mail.nsysu.edu.tw; ctl@ntut.edu.tw; jacky850105@gmail.com

*Abstract*—**The paper studies the estimation of phase noise (PHN) in a full-duplex (FD) orthogonal frequency division multiplexing (OFDM) system. Unlike the conventional half-duplex OFDM system, the receiver faces the challenge of estimating the PHN of the intended signals and self-interference (SI). To address this issue, the PHN estimation problem is transformed into a sparse signal detection problem, which can be solved using compressive sensing techniques. However, the performance of these techniques is limited by linear approximation, improper prior information, or improper structure of the sensing matrix. To overcome these limitations, the extended Kalman filter (EKF) is introduced for PHN estimation. The EKF utilizes the maximum a posteriori probability (MAP) criterion with an approximated linear observation model. Furthermore, a novel MAP estimator is developed that employs the original nonlinear observations. Numerical results validate the effectiveness of the proposed estimators and demonstrate that the proposed MAP estimator outperforms existing compressive sensing approaches due to the utilization of accurate posterior distribution.**

***Index Terms*** **– Full-duplex (FD), orthogonal frequency division multiplexing (OFDM), self-interference (SI), phase noise (PHN), compressive sensing (CS), extended Kalman filter (EKF), maximum a posterior probability (MAP).**

## I. Introduction

Recently, full-duplex (FD) orthogonal frequency division multiplexing systems (OFDM) have been developed to potentially double the spectrum efficiency compared to conventional half-duplex systems [1]. However, FD operation suffers from strong self-interference (SI) due to simultaneous transmission and reception. Therefore, the main task of an FD device is to cancel SI as clearly as possible. However, most existing works mainly address the problem without hardware impairment [2-4]. It is well known that the OFDM system is significantly influenced by hardware impairments. For example, phase noise (PHN) is generated by imperfect pairs of local oscillators at the transmitter and receiver, which destroys the orthogonality between subcarriers and deteriorates performance [5-11].

The estimation of PHN has been investigated for more than two decades for half-duplex OFDM systems [5]-[13]. In [8], the common phase error (CPE) was estimated, which is the dominant part of the PHN and can rotate the channel. The authors in [11] conducted PHN estimation using a maximum likelihood estimator (MLE). In [12], the PHN signal was transferred to lower-dimension representations and was estimated with a least-square (LS) criterion. In millimeter-wave OFDM systems, [7] jointly estimated the PHN and channel. In [5] and [18], the PHN, carrier frequency offset (CFO), and the channel were jointly estimated, where the approximated maximum a posterior probability (MAP) rule was used in [5]. In [6] and [13], the PHN was estimated using the maximum likelihood function with certain geometry constraints of the PHN. The majorization-minimization (MM) technique was then applied to solve the associated optimization problem [6]. Recently, [9] exploited the coherence bandwidth of mmWave systems to approximate the PHN spectrum. Furthermore, in [17], the extended Kalman filter (EKF) was applied to track the PHN of an OFDM system.

In FD-OFDM systems, the received signals contain both intended and SI signals. The PHN can then be generated from two oscillator pairs associated with the intended and SI signals, respectively [16], [19]. In [16], the effect of PHN was analyzed when canceling SI in an FD-OFDM system. In [4], PHNs were incorporated into channels that were modeled as time-varying channels. The basis-expansion model (BEM) was further applied to simplify composite channel estimation. In [19], a similar design was proposed for the FD multiple-input multiple-output (MIMO) OFDM system.

The above studies did not address the task of completely estimating the PHNs raised from the FD-OFDM systems. Motivated by PHN estimation in half-duplex OFDM systems [6], [7], [9], [11], [13], [17], we will study several PHN estimators for FD-OFDM systems and evaluate their performance using computer simulations. The main contributions of our work are summarized as follows:

1. We examine several estimators for two PHNs associated with self-interference (SI) and the intended signals of the separate oscillators used in the transmitter and receiver of an FD-OFDM system.
2. We represent the received signals using sparse representations. We apply several compressive sensing techniques, including the orthogonal matching pursuit (OMP), the iterative soft thresholding algorithm (ISTA), the fast ISTA (FISTA) [14], and the CPE method [15], to conduct PHN estimation.
3. We extend the geometry-preserving PHN estimator (GPE) [13] and the extended Kalman filter (EKF) [18] to perform PHN estimation in FD-OFDM systems.
4. Finally, we propose a maximum a posteriori (MAP)-based PHN estimator and compare its mean-squared error (MSE) performance to other methods. We demonstrate

that the proposed MAP-based PHN estimator outperforms existing methods.

The rest of this paper is organized as follows. In Section II, the received signal model with PHN of the FD-OFDM system is introduced. The PHN estimators are detailed in Section III, where the estimators are realized by the compressive sensing approaches and the MAP rule. In Section IV, we investigate the performance of the proposed design, and finally, the conclusion is drawn in Section V.

Notations: $\mathbf{A}^T$ and $\mathbf{A}^H$ denote the transpose and the conjugate transpose of matrix $\mathbf{A}$, respectively. $\mathbf{x} \odot \mathbf{y}$ represents the point-wise multiplication of $\mathbf{x}$ and $\mathbf{y}$. The notation $\mathbf{x} \sim \mathcal{CN}\left(\mathbf{m}, \mathbf{C}\right)$ indicates that $\mathbf{x}$ is a complex circularly-symmetric Gaussian distributed vector with the mean vector $\mathbf{m}$ and the covariance matrix $\mathbf{C}$. Diag$\{\mathbf{x}\}$ is a diagonal matrix with its diagonal elements from the vector $\mathbf{x}$. vec($\mathbf{A}$) represents collecting the columns of the matrix $\mathbf{A}$ into a vector. $\mathbf{F}$ is the discrete-time Fourier transform (DFT) matrix with $\left[\mathbf{F}\right]_{m,n} = 1/\sqrt{N}e^{-j2\pi mn/N}$. $\mathbf{I}_N$ denotes the $N$x$N$ identity matrix.

## II. System Model

### A. Phase Noise Model

We consider the PHN model of a free-running oscillator: [10]

$$\theta(t) = 2\pi f_0 \eta(t), \tag{1}$$

where $\eta(t)$ is the random time shift process which can be modeled by a Weiner process, and $f_0$ is the oscillator frequency. Therefore, the variant of the phase noise at each sample can be updated by

$$\theta_n = \theta_{n-1} + \varepsilon_n, \tag{2}$$

where $\theta_n$ is the sampled phased noise at the $n$th time instant; $\varepsilon_n$ is the updated error which is an independent and identically distributed Gaussian random variable, i.e., $\varepsilon_n \sim \mathcal{N}\left(0, \sigma_\theta^2\right)$. The variance $\sigma_\theta^2 = 2\pi\beta T_s / N$, where $\beta$ indicates the two-sides 3-dB bandwidth of Lorentzian spectrum of the oscillator. Define $\underline{\theta} = \left[\theta_0 \quad \theta_1 \quad \cdots \quad \theta_{N-1}\right]^T$ as phase noise vector with Gaussian distribution $\mathcal{N}\left(\mathbf{0}, \mathbf{C}_\phi\right)$. By (2), the covariance matrix can be expressed by

$$\left[\mathbf{C}_\phi\right]_{m,n} = \min\left(m, n\right). \tag{3}$$

### B. FD-OFDM System with Phase Noise

We consider a two-way FD-OFDM communication node where each node can concurrently transmit and receive, as shown in Fig. 1. Each node contains two antennas, one for transmission and the other for reception. Define the intended source signals of the $k$th OFDM block as $\mathbf{x}_{S,k}$ = $\left[x_{S,k}[0], \cdots, x_{S,k}[N-1]\right]^T \in \mathbb{C}^{N\times 1}$ where $N$ is the number of subcarriers. The associated transmitted signals after inverse DFT are then read as $\mathbf{s}_k = \mathbf{F}^H \mathbf{x}_{S,k}$. Similarly, we denote $\mathbf{x}_{I,k}$ = $\left[x_{I,k}[0], \cdots, x_{I,k}[N-1]\right]^T \in \mathbb{C}^{N\times 1}$ be the signals transmitted to the destination of the $k$th OFDM block, and the corresponding frequency-domain signals are $\mathbf{d}_k = \mathbf{F}^H \mathbf{x}_{I,k}$. Here, $\mathbf{x}_{I,k}$ is treated as SI.

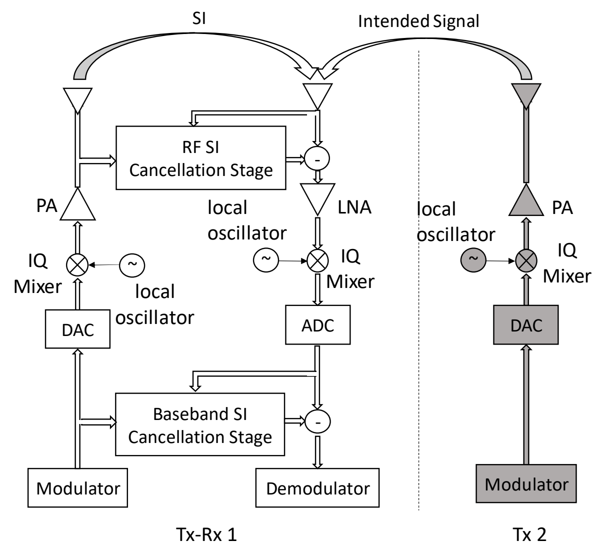


Fig. 1 FD-OFDM communication system.

To prevent inter block interference, the cyclic prefix (CP) with a length longer than the channel delay spread is adopted. The received signals of the $k$th block with PHN after removing CP be given by [9]

$$\mathbf{y}_k = \mathbf{P}_{S,k}\mathbf{H}_{S,k}\mathbf{s}_k + \mathbf{P}_{I,k}\mathbf{H}_{I,k}\mathbf{d}_k + \mathbf{w}_k, \tag{4}$$

where $\mathbf{w}_k \in \mathbb{C}^{N\times 1}$ is the complex Gaussian noise with zero mean and covariance $\sigma_w^2 \mathbf{I}_N$. The first term in (4) presents the signals from the source, which contains the PHN matrix $\mathbf{P}_{S,k}$ = $\mathrm{Diag}\left(\left[e^{j\theta_{S,k,0}}, \cdots, e^{j\theta_{S,k,N-1}}\right]\right)$, $\mathbf{P}_{I,k}$ denotes the PHN resulted from SI signals, given by $\mathbf{P}_{I,k}$ = $\mathrm{Diag}\left(\left[e^{j\theta_{I,k,0}}, \cdots, e^{j\theta_{I,k,N-1}}\right]\right)$. $\left\{\theta_{S,k,i}\right\}$ and $\left\{\theta_{I,k,i}\right\}$ are the global phase processes from the intended signals and the SI, respectively. The global PHN is defined by subtracting the receive PHN from the transmit PHN [4, Eq.6], [16, Eq. 9]. Assume that the intended signal and the SI signals pass through the hardware of different transmit oscillators, the $\left\{\theta_{S,k,i}\right\}$ and $\left\{\theta_{I,k,i}\right\}$ are mutually independent [4], [16, Eq. 9]. Note that $\mathbf{d}_k$ is the transmit signals which is exactly known at the transmitter. After removing the CP, the channel matrix $\mathbf{H}_{S,k}$ is formed of circular structure and can be expressed by

$$\mathbf{H}_{S,k}=\begin{bmatrix} h_{S,k,0} & \cdots & h_{S,k,L_S-1} & h_{S,k,L_S-2} & h_{S,k,1} \\ h_{S,k,1} & h_{S,k,0} & \ddots & \ddots & h_{S,k,L_S-2} \\ \vdots & \ddots & \ddots & \ddots & \vdots \\ \vdots & \ddots & \ddots & \ddots & \vdots \\ h_{S,k,L_S-1} & \cdots & \cdots & \cdots & h_{S,k,0} \end{bmatrix}^T \tag{5}$$

and $h_{S,k,i}$, $i = 0,\ldots, L_S$, is the multipath corresponding to the source. Similarly, we have $\mathbf{H}_{I,k}$ is formed by

$$\mathbf{H}_{I,k}=\begin{bmatrix} h_{I,k,0} & \cdots & h_{I,k,L_I-1} & h_{I,k,L_I-2} & h_{I,k,1} \\ h_{I,k,1} & h_{I,k,0} & \ddots & \ddots & h_{I,k,L_I-2} \\ \vdots & \ddots & \ddots & \ddots & \vdots \\ \vdots & \ddots & \ddots & \ddots & \vdots \\ h_{I,k,L_I-1} & \cdots & \cdots & \cdots & h_{I,k,0} \end{bmatrix}^T \tag{6}$$

## III. PHASE NOISE ESTIMATION

### A. PHN Estimation with Sparse Property

Our goal is to estimate the PHNs $\left\{\theta_{S,k,i}\right\}$ and $\left\{\theta_{I,k,i}\right\}$ by the observation (4). Assume the signals $\mathbf{s}_k$, channels $\mathbf{H}_{S,k}$ and $\mathbf{H}_{I,k}$ are perfectly known [11], we can reformulate (4) as a concise linear receive model

$$\begin{aligned}\mathbf{y}_k &= \mathbf{P}_{S,k}\mathbf{H}_{S,k}\mathbf{s}_k + \mathbf{P}_{I,k}\mathbf{H}_{I,k}\mathbf{d}_k + \mathbf{w}_k \\ &= \mathbf{a}_{S,k}\odot\mathbf{p}_{S,k} + \mathbf{a}_{I,k}\odot\mathbf{p}_{I,k} + \mathbf{w}_k\end{aligned} \tag{7}$$

where $\mathbf{a}_{S,k}=\mathbf{H}_{S,k}\mathbf{s}_k$ and $\mathbf{a}_{I,k}=\mathbf{H}_{I,k}\mathbf{d}_k$ ; $\mathbf{p}_{S,k}=\exp\left(j\underline{\theta}_{S,k}\right)$, $\mathbf{p}_{I,k}=\exp\left(j\underline{\theta}_{I,k}\right)$ with $\underline{\theta}_{S,k}=\left[\theta_{S,k,0},\cdots,\theta_{S,k,N-1}\right]$ and $\underline{\theta}_{I,k}=\left[\theta_{I,k,0},\cdots,\theta_{I,k,N-1}\right]$ being the global PHNs resulted from the intended signals and the SI, respectively. Without loss of generality, we assume the variance of the innovation error in $\underline{\theta}_{S,k}$ and $\underline{\theta}_{I,k}$ is $\sigma_\theta^2$. Since the PHNs $\left\{\theta_{S,k,i}\right\}$ and $\left\{\theta_{I,k,i}\right\}$ follow the first-order Weiner process (2) with small variance, (7) can be transferred to a sparse representation given by

$$\mathbf{y}_k=\overline{\mathbf{A}}_k\mathbf{c}_k+\mathbf{w}_k, \tag{8}$$

where

$$\overline{\mathbf{A}}_k=\left[\mathrm{Diag}\left\{\mathbf{a}_{S,k}\mathbf{F}^H\right\}\quad \mathrm{Diag}\left\{\mathbf{a}_{I,k}\mathbf{F}^H\right\}\right], \tag{9}$$

and

$$\mathbf{c}_k=\begin{bmatrix}\mathbf{F}\mathbf{p}_{S,k}\\ \mathbf{F}\mathbf{p}_{I,k}\end{bmatrix} \tag{10}$$

is the sparse signal we want to estimate. Intuitively, estimating $\mathbf{c}_k$ in Eq. (8) represents a compressive sensing problem with the sensing matrix $\overline{\mathbf{A}}_k$. Therefore, the OMP, ISTA, and FISTA [14] can be applied to estimate $\mathbf{c}_k$. However, the structure of the sensing matrix is under restricted isometry property (RIP) to achieve better performance for the OMP algorithm. The ISTA and FISTA realize a low-complexity ML detection for (8) with sparse prior information.

### B. PHN Estimator with Extended Kalman Filter (EKF)

Note that Eq. (8) is a linear function of $\mathbf{c}_k$ but not a linear function of $\underline{\theta}_k=\left[\underline{\theta}_{S,k}^T\quad \underline{\theta}_{I,k}^T\right]^T$. In this regard, the linear Taylor approximation is used in EKF to sequentially detect each element of $\underline{\theta}_k$ by considering the Gaussian distributed variations of the PHN model in (8) [17], [18]. Nevertheless, the mismatch between the original nonlinear model and the approximated linear one by the first-order Taylor expansion leads to correlated modeling errors, which also degrades the estimation performance, particularly for the large dimensional received signal. Therefore, in the next subsection, we proposed an alternative approach to realize the PHN estimation with MAP criterion.

### C. Proposed MAP-based PHN Estimator

In this subsection, we will directly adopt the MAP estimator to estimate $\underline{\theta}_k$. Toward this end, we first decide the posterior distribution by the Bayesian rule:

$$p\left(\mathbf{p}_k\left|\mathbf{y}_k,\mathbf{A}_k\right.\right)\propto p\left(\mathbf{y}_k\left|\mathbf{p}_k,\mathbf{A}_k\right.\right)p\left(\underline{\theta}_k\right), \tag{11}$$

where the likelihood function $p\left(\mathbf{y}_k\left|\mathbf{p}_k,\mathbf{A}_k\right.\right)$ is expressed by

$$p\left(\mathbf{y}_k\left|\mathbf{p}_k,\mathbf{A}_k\right.\right)\propto\exp\left(-\sigma_w^{-2}\left\|\mathbf{y}_k-\mathbf{A}_k\mathbf{p}_k\right\|^2\right) \tag{12}$$

and $p\left(\underline{\theta}_k\right)$ is the prior distribution of the PHN vector $\underline{\theta}_k$ and is expressed by

$$\begin{aligned}p\left(\underline{\theta}_k\right)&=p\left(\underline{\theta}_{S,k}\right)p\left(\underline{\theta}_{I,k}\right)\\ &\propto\exp\left(-\frac{\left(\theta_{S,k,0}-\theta_{S,k-1,N-1}\right)^2}{2N_{CP}\sigma_\theta^2}-\sum_{i=1}^{N-1}\frac{\left(\theta_{S,k,i}-\theta_{S,k,i-1}\right)^2}{2\sigma_\theta^2}\right)\\ &\quad\exp\left(-\frac{\left(\theta_{I,k,0}-\theta_{I,k-1,N-1}\right)^2}{2N_{CP}\sigma_\theta^2}-\sum_{i=1}^{N-1}\frac{\left(\theta_{I,k,i}-\theta_{I,k,i-1}\right)^2}{2\sigma_\theta^2}\right).\end{aligned} \tag{13}$$

Hererin, $\theta_{S,k-1,N-1}$ and $\theta_{I,k-1,N-1}$ represent the last PHN in the ($k$-1)th OFDM symbol. It is noteworthy that $\theta_{S,k,0}$ ($\theta_{I,k,0}$) possesses the larger value of variance due to the fact that the $N_{CP}$ sampling points of cyclic prefix (CP). Accordingly, the estimation of $\underline{\theta}_k$ by MAP can thus be conducted by the following optimization problem:

$$\min_{\{\theta_{S,k,i}\},\{\theta_{I,k,i}\}} f\left(\underline{\theta}_k\right) \tag{14}$$

where the cost function $f\left(\underline{\theta}_k\right)$ corresponds to the $\ln p\left(\underline{\theta}_k\right)$ and is given by

$$\begin{aligned} f\left(\underline{\theta}_k\right) &= \sigma_w^{-2}\left\|\mathbf{y}_k - \mathbf{a}_{S,k}\odot\mathbf{p}_{S,k} - \mathbf{a}_{I,k}\odot\mathbf{p}_{I,k}\right\|^2 + \\ &\frac{\left(\theta_{S,k,0}-\theta_{S,k-1,N-1}\right)^2}{2N_{CP}\sigma_\theta^2} + \sum_{i=1}^{N-1}\frac{\left(\theta_{S,k,i}-\theta_{S,k,i-1}\right)^2}{2\sigma_\theta^2} \\ &\frac{\left(\theta_{I,k,0}-\theta_{I,k-1,N-1}\right)^2}{2N_{CP}\sigma_\theta^2} + \sum_{i=1}^{N-1}\frac{\left(\theta_{I,k,i}-\theta_{I,k,i-1}\right)^2}{2\sigma_\theta^2}. \end{aligned} \tag{15}$$

In light of the MAP estimator of (14), we have the following observations. The estimation is dominated by two parts, the likelihood part and the prior information part. The prior information part describes the correlation between the PHN where the smaller value of $\sigma_\theta^2$, the higher correlation they have. Transferring the PHN into the frequency domain, the signal turns out to be sparse, and the value is concentrated in the direct component (DC). Hence, the sparse signals are not independent and identically distributed (i.i.d.). In addition, the likelihood part dominates the estimation of PHN in high SNR region ($\sigma_w^2$ is small). However, the likelihood function is not convex in $\left\{\theta_{S,k,i}\right\}$ and $\left\{\theta_{I,k,i}\right\}$, which is difficult in finding the optimal solution.

To solve (14), we adopt the gradient descent method to find a local solution. Therefore, the main task is to compute the gradient of $f\left(\underline{\theta}_k\right)$ with respect to $\underline{\theta}_{S,k}$ and $\underline{\theta}_{I,k}$. After some manipulations, the gradient of $f\left(\underline{\theta}_k\right)$ can be computed as

$$\begin{aligned} \nabla_{\underline{\theta}_{S,k}} f\left(\underline{\theta}_k\right) &= 2\sigma_w^{-2}\left(\mathrm{Im}\left\{\mathbf{y}_k^*\odot\mathbf{p}_{S,k}\odot\mathbf{a}_{S,k}\right\}\right. \\ &\left.+\,\mathrm{Im}\left\{\mathbf{p}_{S,k}^*\odot\mathbf{a}_{S,k}^*\odot\mathbf{p}_{I,k}\odot\mathbf{a}_{I,k}\right\}\right) + \sigma_\phi^{-2}\mathbf{g}_{\theta,S,k} \end{aligned} \tag{16}$$

$$\begin{aligned} \nabla_{\underline{\theta}_{I,k}} f\left(\underline{\theta}_k\right) &= 2\sigma_w^{-2}\left(\mathrm{Im}\left\{\mathbf{y}_k^*\odot\mathbf{p}_{I,k}\odot\mathbf{a}_{I,k}\right\}\right. \\ &\left.+\,\mathrm{Im}\left\{\mathbf{p}_{I,k}^*\odot\mathbf{a}_{I,k}^*\odot\mathbf{p}_{S,k}\odot\mathbf{a}_{S,k}\right\}\right) + \sigma_\phi^{-2}\mathbf{g}_{\theta,I,k} \end{aligned} \tag{17}$$

with

$$\mathbf{g}_{\theta,S,k} = \begin{bmatrix} N_{CP}^{-1}\left(\theta_{S,k,0}-\theta_{S,k-1,N-1}\right)-\left(\theta_{S,k,1}-\theta_{S,k,0}\right) \\ \sigma_\theta^{-2}\left(2\theta_{S,k,1}-\theta_{S,k,0}-\theta_{S,k,2}\right) \\ \vdots \\ \sigma_\theta^{-2}\left(2\theta_{S,k,i}-\theta_{S,k,i-1}-\theta_{S,k,i+1}\right) \\ \vdots \\ \sigma_\theta^{-2}\left(\theta_{S,k,N-1}-\theta_{S,k,N-2}\right) \end{bmatrix} \tag{18}$$

$$\mathbf{g}_{\theta,I,k} = \begin{bmatrix} N_{CP}^{-1}\left(\theta_{I,k,0}-\theta_{I,k-1,N-1}\right)-\left(\theta_{I,k,1}-\theta_{I,k,0}\right) \\ \sigma_\theta^{-2}\left(2\theta_{I,k,1}-\theta_{I,k,0}-\theta_{I,k,2}\right) \\ \vdots \\ \sigma_\theta^{-2}\left(2\theta_{I,k,i}-\theta_{I,k,i-1}-\theta_{I,k,i+1}\right) \\ \vdots \\ \sigma_\theta^{-2}\left(\theta_{I,k,N-1}-\theta_{I,k,N-2}\right) \end{bmatrix} \tag{19}$$

Then, the PHN of the *k*th time instant can be iteratively solved by

$$\underline{\theta}_k^{(i+1)} = \begin{bmatrix}\underline{\theta}_{S,k}^{(i+1)} \\ \underline{\theta}_{I,k}^{(i+1)}\end{bmatrix} = \underline{\theta}_k^{(i)} - \mu\begin{bmatrix}\nabla_{\underline{\theta}_{S,k}} f\left(\underline{\theta}_k^{(i)}\right) \\ \nabla_{\underline{\theta}_{I,k}} f\left(\underline{\theta}_k^{(i)}\right)\end{bmatrix}, \tag{20}$$

where $\mu$ is the step size, and the superscript ($i$) represents the $i$th iteration. The PHNs can be obtained until the iterations in (20) converge. Generally, the performance of the gradient descent method is sensitive to its initial value when the problem is not convex. A proper initial value can not only reach to a better local solution but accelerate the convergence. Herein, we adopt the estimation result in [18] as our initial estimation.

## IV. SIMULATION RESULTS

In this section, we evaluate the performance of the proposed PHN estimation in an FD-OFDM system. Herein, we assume that the number of subcarriers is $N$=128. The PHN estimation is conducted in the training phase, where the signal vectors $\mathbf{s}_k$ and $\mathbf{d}_k$ are modulated with QPSK and are known at the receiver. The circular channel matrices of $\mathbf{H}_{S,k}$ and $\mathbf{H}_{I,k}$ are generated by Rayleigh distribution and are assumed to be perfectly known at the receiver. Without loss of generality, we assume the power of each element of $\mathbf{H}_{S,k}$ and $\mathbf{H}_{I,k}$ is identical. The MSE is evaluated by summation of MSE resulted from both $\hat{\underline{\theta}}_{S,k}$ and $\hat{\underline{\theta}}_{I,k}$, i.e., $E\left[\left\|\hat{\underline{\theta}}_{S,k}-\underline{\theta}_{S,k}\right\|^2\right]$ + $E\left[\left\|\hat{\underline{\theta}}_{I,k}-\underline{\theta}_{I,k}\right\|^2\right]$. Several estimation approaches are compared, including ISTA, FISTA, OMP [14], the CPE estimator [15], the GPE [13], the EKF [18], and the proposed MAP design.

Fig. 2 shows the MSE performance of PHN estimation with $\sigma_\theta^2 = 10^{-3}$. As seen, the performance of CPE [15] is saturated because it only estimates the direct component (DC) of the PHN. The residual frequency components of the PHN cause inter-carrier interference (ICI). In contrast, GPE [13], ISTA, FISTA, and OMP [14] estimate the complete PHN using additional prior information of the sparse property. Hence, their performances are superior to [15]. Furthermore, the OMP method performs poorly in the low SNR region due to the poor isometry property of the associated sparse sensing matrix in (9). However, the ISTA, FISTA, and GPE methods can improve performance by utilizing additional sparse information in the optimization process. Finally, we observe that the EKF and the proposed MAP outperform the others. This is because the OMP, ISTA, FISTA, and GPE methods optimize the likelihood function with various types of sparse prior information, whereas the EKF and the proposed MAP are developed using the MAP rule directly. The proposed MAP method is superior to the EKF method as the EKF approximates the posterior distribution as Gaussian, while the proposed MAP uses the accurate posterior distribution to conduct the MAP estimator, thus outperforming the others.

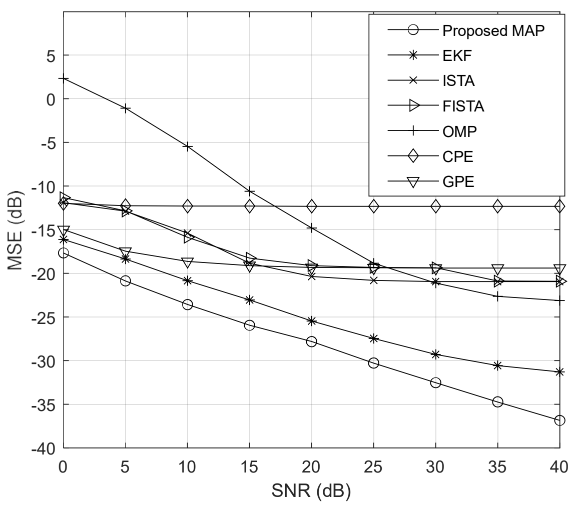


Fig. 2 The MSE versus the SNR with different PHN estimators.

## V. CONCLUSIONS

In this paper, several PHN estimators were investigated for an FD-OFDM system. The received signals with PHN were first reformulated as sparse signal representations. Compressive sensing approaches such as OMP, ISTA, and FISTA were applied to estimate the PHN. Additionally, the geometry-preserving PHN (GPN) constraint was utilized to improve accuracy of PHN estimation. In addition to these compressive sensing techniques, the EKF was employed to estimate the PHN using an approximated Gaussian posterior distribution. Finally, a MAP-based PHN estimation approach was proposed that leverages an accurate posterior distribution. Simulation results validate the studied PHN estimators and demonstrate the superiority of the proposed MAP-based estimator.

## REFERENCES


[1] W. Li, J. Lilleberg, K. Rikkinen, “On rate region analysis of half- and full-duplex OFDM communication links,” *IEEE Journal on Selected Areas in Commun.*, vol. 32, no. 9, pp. 1688-1698, Sept. 2014.

[2] Z. Zhan and G. Villemaud, “Combination of digital self-interference cancellation and AARFSIC for Full-Duplex OFDM wireless,” in *Proc. IEEE ICCC 2014*.

[3] C.-W. Jen, H.-W. Yang, H.-W. Chan, H.-C. Liu, H. Lopez, C.-Y. Liu, and S.-J. Jou, “Digital self-interference cancellation for OFDM full-duplex transmission in 60 GHz band,” in *Proc. IEEE ISCAS 2018*.

[4] R. Li, A. Masmoudi , and T. Le-Ngoc, "Self-interference cancellation with nonlinearity and phase-noise suppression in full-duplex systems," *IEEE Trans. Veh. Tech*., vol. 67, no. 3, pp. 2118-2129, March 2018.

[5] D. D. Lin, R. A. Pacheco, T. J. Lim, and D. Hatzinakos, “Optimal OFDM channel estimation with carrier frequency offset and phase noise,” in *Proc. IEEE WCNC 2006*.

[6] Z. Wang, P. Babu, and D. P. Palomar, “Effective low-complexity optimization methods for joint phase noise and channel estimation in OFDM,” *IEEE Trans. Signal Process.*, vol. 65, no. 12, pp. 3247-3260, June 2017.

[7] S. Suyama, H. Suzuki, K. Fukawa, and J. Izumi, “Iterative receiver employing phase noise compensation and channel estimation for millimeter-wave OFDM systems,” *IEEE J. Sel. Areas Commun.*, vol. 27, no. 8, pp. 1358–1366, Sep. 2009.

[8] G. Liu and W. Zhu, “Compensation of phase noise in OFDM systems using an ICI reduction scheme,” *IEEE Trans. Broadcast.*, vol. 50, no. 4, pp. 399–407, Dec. 2004.

[9] M. Chung, L. Liu, and O. Edfors, “Phase-noise compensation for OFDM systems exploiting coherence bandwidth: Modeling, algorithms, and analysis,” *IEEE Trans. Commum.*, vol. 21, no. 5, pp. 3040-3056, May 2022.

[10] A. Demir, A. Mehrotra, and J. Roychowdhury, “Phase noise in oscillators: A unifying theory and numerical methods for characterization,” IEEE Transactions on Circuits and Systems I: Fundamental Theory and Applications,” vol. 47, no. 5, pp. 655–674, May 2000.

[11] S. Wu, P. Liu, and Y. Bar-Ness, “Phase noise estimation and mitigation for OFDM systems,” *IEEE Trans. Wireless Commum.*, vol. 5, no. 12, pp. 3616-3625, Dec. 2006.

[12] A. Leshem and M. Yemini, “Phase Noise Compensation for OFDM Systems,” *IEEE Trans. Signal Process*., vol. 65, no. 21, pp. 5675-5686, Nov. 2017.

[13] P. Mathecken, T. Riihonen, and R. Wichman, “Constrained phase noise estimation in OFDM using scattered pilots without decision feedback,” *IEEE Trans. Signal Process.*, vol. 65, no. 9, pp. 2348-2362, May 2017.

[14] Z. Zhang, Y. Xu, J. Yang, X. Li and D. Zhang, “A survey of sparse representation: Algorithms and applications,” *IEEE Access*, vol. 3, pp. 490-530, May. 2015.

[15] T.-J. Lee and Y. C. Ko, “Channel estimation and data detection in the presence of phase noise in MIMO-OFDM systems with independent oscillators,” *IEEE Access*, vol. 5, pp. 9647-9661, 2017.

[16] V. Syrjala, M. Valkama, L. Anttila, T. Riihonen, and D. Korpi,” Analysis of oscillator phase-noise effects on self-interference cancellation in full-duplex OFDM radio transceivers,” *IEEE Trans. Wireless Commun.*, vol. 13, no. 6, pp. 2977-2990, June 2014.

[17] M. Bensan, V. P. S. Kirar, and K. Burse, “Phase noise reduction and tracking in OFDM using extended kalman filter,” in Proc. *2012 Fourth International Conference on Computational Intelligence and Communication Networks*.

[18] O. H. Salim, A. A. Nasir, H. Mehrpouyan, W. Xiang, S. Durrani, and R. A. Kennedy, “Channel, phase noise, and frequency offset in OFDM systems: Joint estimation, data detection, and hybrid Cramér-Rao lower bound,” *IEEE Trans. Commun.*, vol. 62, no. 9, pp. 3311-3325, Sept 2014.

[19] N. D. N. Vien, B. T. M. Tu, T. T. Vhien, N. Q. B. Vo, N. L. Hung, "Joint phase noise and doubly selective channel estimation in full-duplex MIMO-OFDM systems" in *Proc. IEEE ATC 2016*.